



Published in final edited form as:

*Exp Hematol.* 2019 February ; 70: 70–84.e6. doi:10.1016/j.exphem.2018.11.008.

## ***Smc3* is required for mouse embryonic and adult hematopoiesis**

Tianjiao Wang<sup>1</sup>, Brandi Glover<sup>1</sup>, Gayla Hadwiger<sup>1</sup>, Christopher A. Miller<sup>1,2</sup>, Orsola di Martino<sup>1</sup>, and John S. Welch<sup>1</sup>

<sup>1</sup>Department of Internal Medicine, Washington University School of Medicine, St. Louis, Missouri

<sup>2</sup>McDonnell Genome Institute, Washington University School of Medicine, Saint Louis, MO

### **Abstract**

*SMC3* encodes a subunit of the cohesin complex that has canonical roles in regulating sister chromatids segregation during mitosis and meiosis. Recurrent heterozygous mutations in *SMC3* have been reported in acute myeloid leukemia (AML) and other myeloid malignancies. In this study, we investigated whether the missense mutations in *SMC3* might have dominant-negative effects or phenocopy loss-of-function effects by comparing the consequences of *Smc3* deficient and haploinsufficient mouse models. We found that homozygous deletion of *Smc3* during embryogenesis or in adult mice led to hematopoietic failure, suggesting that *SMC3* missense mutations are unlikely to be associated with simple dominant negative phenotypes. In contrast, haploinsufficiency was tolerated during embryonic and adult hematopoiesis. Under steady-state conditions, *Smc3* haploinsufficiency did not alter colony forming in methylcellulose, only modestly decreased mature myeloid cell populations, and led to limited expression changes and chromatin alteration in Lin-cKit<sup>+</sup> bone marrow cells. However, following transplantation, engraftment, and subsequent deletion, we observed a hematopoietic competitive disadvantage across myeloid and lymphoid lineages and within the stem/progenitor compartments. This disadvantage was not affected by hematopoietic stresses but was partially abrogated by concurrent *Dnmt3a* haploinsufficiency, suggesting that antecedent mutations may be required to optimize the leukemogenic potential of *Smc3* mutations.

### **Introduction**

Acute myeloid leukemia (AML) is an aggressive hematopoietic malignancy, characterized by the accumulation of myeloblasts in the blood or bone marrow (BM) with maturation arrest and retained self-renewal.<sup>1</sup> Tremendous progress has been made in identifying

Correspondence: John S. Welch, MD/PhD, jwelch@wustl.edu, Division of Oncology, 660 South Euclid Ave, Box 8007, St. Louis, MO 63110.

Author contributions

TW and JSW designed experiments, performed experiments, interpreted data, and wrote the paper. BG, GH, CAM, and ODM performed experiments and interpreted data.

**Publisher's Disclaimer:** This is a PDF file of an unedited manuscript that has been accepted for publication. As a service to our customers we are providing this early version of the manuscript. The manuscript will undergo copyediting, typesetting, and review of the resulting proof before it is published in its final citable form. Please note that during the production process errors may be discovered which could affect the content, and all legal disclaimers that apply to the journal pertain.

The authors have declared that no conflict of interest exists.

recurrent gene mutations in AML, yet we are still in the early stages of understanding the mechanisms through which these genetic alterations contribute to the onset of the disease.<sup>2</sup>

Recurring mutations in the cohesin complex occur in four core components, *SMC3*, *SMC1A*, *RAD21*, and *STAG2*, and have been identified in AML and other myeloid malignancies.<sup>3, 4, 5</sup> Over 50% of patients with Down syndrome-associated acute megakaryocytic leukemia (DS-AMKL) have cohesin mutations, specifically in *STAG2*.<sup>6</sup> Somatic cohesin mutations have also been observed in a variety of solid cancers, including colorectal carcinoma, ovarian carcinoma, glioblastoma, bladder carcinoma, and Ewing's sarcoma.<sup>7, 8, 9, 10, 11, 12</sup> Additionally, germline mutations of the cohesin complex are causally related to developmental disorders, particularly cohesinopathies such as Cornelia de Lange syndrome (CdLS).<sup>13, 14</sup>

*SMC3* and *RAD21* mutations are nearly universally heterozygous, whereas mutations in *SMC1A* and *STAG2* may be hemizygous because they are X-linked. Cohesin mutations also tend to be mutually exclusive, implying that alteration in one component may be sufficient to disrupt the entire complex or alternatively, they may not be tolerated by a cell when co-occurring.<sup>15, 16</sup> Cohesin mutations are often observed as early subclonal events in AML, conceivably facilitating disease initiation, although they are not observed in cases of clonal hematopoiesis of indeterminate potential (CHIP), suggesting they are unlikely to be the initiating event.<sup>15, 17, 18, 19</sup>

The majority of *SMC3* mutations are missense mutations; only one-third of *SMC3* mutations are nonsense or splice-site variants. The missense mutations are scattered across all domains, although a few recurrently mutated nucleotides have been observed (R381Q, R661P). This pattern suggests that many of these mutations may result in simple loss-of-function consequences, although novel dominant negative activities cannot be dismissed within the hot-spot variants. Intriguingly, *DNMT3A* mutations, one of the most commonly mutated genes in AML, frequently coincided with *SMC3* mutations, suggesting there may be leukemogenic interactions between these mutations.<sup>5, 15, 16, 20</sup>

In yeast and cell line-based studies, cohesin has been shown to play essential roles in sister chromatid segregation during cell cycle, DNA damage repair, transcriptional regulation via chromatin looping, and maintenance of chromatin architecture.<sup>21, 22, 23, 24</sup> Notably, AML patients who harbor cohesin mutations typically have normal karyotype, indicating that hematopoietic cohesin mutations do not lead directly to chromosomal instability.<sup>25, 16</sup>

To define the hematopoietic consequences of *SMC3* mutations and to determine whether these could reflect dominant negative or loss of function phenotypes, we characterized the *in vivo* effects of *Smc3* deficiency and *Smc3* haploinsufficiency on murine hematopoiesis using conditionally deleted strategies. In contrast to our expectations that these leukemia-associated mutations would lead to expansions of hematopoietic stem cell populations or augmented self-renewal, we observed a competitive disadvantage in *Smc3* deficient and haploinsufficient BM cells *in vivo* without an associated increase in maturation-arrested stem cells.

## Results

### Generation of *Smc3* conditional knockout mice

To investigate the effects of *Smc3* loss on hematopoiesis, we generated *Smc3* conditionally deficient and haploinsufficient mice using *Smc3*<sup><tm1a(EUCOMM)Wtsi></sup> mice obtained from EUCOMM (*Smc3*<sup>trap</sup>). The *Smc3*<sup>trap</sup> allele has a lacZ-neomycin-gene-trap cassette inserted in intron 4 with two Frt sites on each side of the cassette, and two loxP sites flanking exon 4. The gene trap is predicted to lead to an early transcription stop after splicing into lacZ-neomycin. The conditional knockout *Smc3*<sup>fl</sup> allele was created by excising the gene-trap cassette with Flp recombinase and was used for further characterizations because homozygous deletion could be achieved using the *Smc3*<sup>fl</sup> allele (Figure 1A). We validated the integration of the loxP sites surrounding exon 4 in the *Smc3*<sup>fl</sup> allele using whole genome sequencing (Figure 1B).

We examined the transcriptional consequences of the *Smc3*<sup>fl</sup> allele using RNA-Seq and intracellular flow cytometry. In BM cells from three *Smc3*<sup>fl/+</sup>/*Vav1-Cre*<sup>+/-</sup> mice, nearly 50% (48.4%) of transcripts spliced from exon 3 to exon 5, consistent with deletion of exon 4 while all the wild-type transcripts spliced from exon 3 to exon 4 and exon 4 to exon 5 (Figure 1C and Supplemental Figure 1A–F). Analysis of reads spanning exons 3–5 suggests that this results in a frameshift mutation and a stop codon after 59 amino acids, although this truncated protein could not be detected using N-terminal antibodies. Using C-terminal antibodies, intracellular Smc3 protein level was reduced to approximately half of littermate control, as would be expected with a heterozygous allele and confirming *Smc3* haploinsufficiency (Figure 1D). In addition, we noted that Smc3 protein level was regulated during normal hematopoiesis, with higher expression in KLS (Lin-cKit+Sca1+) stem/progenitor cells vs. SLAM (Lin-cKit+Sca1+CD150+CD48-) stem cells (Figure 1E). Representative primary intracellular flow data shown in Supplemental Figure 2.

### Homozygous *Smc3* deletion

To understand whether *SMC3* mutations might have dominant-negative effects or phenocopy loss-of-function effects, we compared the consequences of *Smc3* deficient and haploinsufficient mouse models. We found that hematopoietic homozygous deletion of *Smc3* led to embryonic lethality. In heterozygous *Smc3*<sup>fl/+</sup>/*Vav1-Cre*<sup>+/-</sup> intercrosses, we observed 0 out of 75 pups with homozygous *Smc3* alleles (Figure 2A). To determine whether the cause of death in *Smc3*<sup>fl/fl</sup>/*Vav1-Cre*<sup>+/-</sup> embryos was from hematopoietic failure, we examined E13.5 embryos. Grossly, the *Smc3*<sup>fl/fl</sup>/*Vav1-Cre*<sup>+/-</sup> embryos were indistinguishable in size and appearance from other genotypes, except the lack of obvious fetal livers (Figure 2B–C). A severe decrease in fetal liver hematopoietic cells was verified by cell count and flow cytometry with near-complete absence of CD45+ Gr1+ CD11b+ cells demonstrating myeloid-biased hematopoietic failure (Figure 2DF).

We investigated somatic homozygous *Smc3* deletion in adult mice using the *Smc3*<sup>fl/fl</sup>/*ERT2-Cre*<sup>+/-</sup> mice. *Smc3* deletion was achieved by treating mice with oral tamoxifen (TAM) at 6 weeks of age and reduction in Smc3 protein confirmed with western blot (Supplemental Figure 3A). After 4 doses of TAM, mice were moribund and therefore sacrificed for

analysis. Complete blood counts (CBC) data showed the *Smc3<sup>fl/fl</sup>/ERT2-Cre<sup>+/-</sup>* mice had lower white blood cell counts, percentages of lymphocytes, neutrophils, and monocytes, and fewer platelets than TAM-treated littermates (Figure 3A). The *Smc3<sup>fl/fl</sup>/ERT2-Cre<sup>+/-</sup>* mice had decreased spleen weights (Figure 3B) and their spleens were smaller in size (Supplemental Figure 3B). Total number of cells in BM, spleen, and thymus of the *Smc3<sup>fl/fl</sup>/ERT2-Cre<sup>+/-</sup>* mice were significantly reduced in comparison to *Smc3<sup>fl/fl</sup>* mice after TAM treatment (Figure 3C). The reduction of cells occurred across all lineages in the BM (Figure 3D), spleen, and thymus (Supplemental Figure 3C–D) of the *Smc3<sup>fl/fl</sup>/ERT2-Cre<sup>+/-</sup>* mice, suggesting complete hematopoietic collapse.

Because activation of ERT2-Cre leads to *Smc3* deletion in a wide range of cells and tissues, we repeated these studies, isolating hematopoietic cells via a competitive transplantation. Equivalent engraftment of transgenic CD45.2+ and competitor CD45.1+ CD45.2+ cells was verified 6 weeks after transplantation. Following tamoxifen-induced *Smc3* deletion, the *Smc3<sup>fl/fl</sup>/ERT2-Cre<sup>+/-</sup>* donor cells were quickly outcompeted, indicating complete loss of hematopoietic stem and progenitor cell (HSPC) functions in the *Smc3<sup>fl/fl</sup>/ERT2-Cre<sup>+/-</sup>* BM. Once again, the effect was most pronounced within the myeloid compartment (Figure 3E–F), suggesting that myeloid hematopoiesis is sensitive to *Smc3* deletion and therefore, the AML-associated *SMC3* mutations are unlikely to have simple dominant-negative effects.

### Steady-state heterozygous *Smc3* deletion

In the ExAC database ([exac.broadinstitute.org](http://exac.broadinstitute.org)), no *SMC3* loss-of-function mutations are observed in available human data (0 observed vs. 58.5 expected mutations), suggesting potential embryonic lethality or reduced fitness associated with *Smc3* haploinsufficiency. We, therefore, determined whether *Smc3* haploinsufficiency might be tolerated in mice. Because *CMV-Cre* is X-linked and expressed during early embryogenesis, we examined the ratio of male: female pups and compared difference between genders to determine whether embryonic *Smc3* haploinsufficiency altered hematopoiesis. We found that *Smc3* haploinsufficiency led to a normal number of female pups in *CMV-Cre* intercrosses (Supplemental Figure 4A), and the female pups had no obvious defects in complete blood counts, total number of BM cells, and percentages of HSPCs and cells in different lineages (Supplemental Figure 4B–E). Hence, embryonic *Smc3* haploinsufficiency could be tolerated and did not grossly perturb steady-state hematopoiesis in mice.

We next assessed the effects of somatic *Smc3* haploinsufficiency on hematopoiesis using the inducible *Smc3<sup>fl/+</sup>/ERT2-Cre<sup>+/-</sup>* mice. *Smc3* haploinsufficiency did not alter the proportions of immunophenotypic HSPCs and cells of different lineages (Figure 4A–B).

Furthermore, *Smc3* haploinsufficiency did not increase the number of colonies formed in methylcellulose or the average number of cells per colony, and the *Smc3* haploinsufficient BM cells did not replat beyond two weeks (Figure 4C–E). At the end of each week, the colonies on each plate were collected, washed, and characterized by immunophenotype. At the end of week 1, the cells were predominantly Gr1+ CD11b+ for both *Smc3<sup>fl/+</sup>/ERT2-Cre<sup>+/-</sup>* and *Smc3<sup>fl/+</sup>* genotypes. However, starting week 2, the colonies shifted to cKit+ FcER1+ mast cells. In week 3 and 4, the few colonies left were exclusively mast cells (Supplemental

Figure 5A–B). Similar results were observed using BM cells from *Smc3<sup>fl/+</sup>/Vav1-Cre<sup>+/-</sup>* mice.

We performed RNA-Sequencing to measure global gene expression in *Smc3* haploinsufficient hematopoietic progenitors (Lin-cKit+Sca1-) using the constitutive *Smc3<sup>fl/+</sup>/Vav1-Cre<sup>+/-</sup>* model. This model was chosen because it required minimal manipulation of the mice, provided hematopoietic-restricted deletion, and would evaluate steady-state hematopoietic conditions. Multipotent progenitors (KLs) were sorted from age-matched individual wild-type and *Smc3<sup>fl/+</sup>/Vav1-Cre<sup>+/-</sup>* mice for RNA-Seq. KLs were selected because *Smc3* haploinsufficiency resulted in severe multi-lineage competitive disadvantage *in vivo*, suggesting potential defect in the functions of *Smc3* haploinsufficient KLs. However, minimal global transcriptional changes were detected. Using t-tests and Significance Analysis of Microarrays (SAM)<sup>26</sup> 149 genes were identified with differential expression in *Smc3* haploinsufficient KLs in comparison to wild-type controls (most with < 2 fold changes) (Figure 4F). KEGG pathway analysis showed significance ( $p < 0.002$  and  $p < 0.005$ ) for progesterone mediate oocyte maturation and toxoplasmosis respectively, but these are not related to hematopoiesis.<sup>27</sup> *Smc3* expression was not observed to be different when analyzed using total reads across the entire gene. However, we observed a two-fold reduction in expression of exon 4 consistent with deletion of this exon (Figure 1C).

To determine whether *Smc3* haploinsufficiency might lead to alterations in global chromatin structure that may be biologically relevant, but which did not lead to measurable altered gene transcription, we performed transposase-accessible chromatin sequencing (ATAC-Seq). Chromatin accessibility peaks of the *Smc3<sup>fl/+</sup>/Vav1-Cre<sup>+/-</sup>* KLs and littermate *Smc3<sup>fl/+</sup>* controls revealed by ATAC-Seq were not significantly different except for peaks in proximity of three genes: *Vav1*, *Tnpo3*, *Tgfb* (Figure 4G). The two-fold difference in *Vav1* was expected for the heterozygous allele and therefore indicated fidelity of data generated by the assay.

### Phenotypes of *Smc3* haploinsufficiency following competitive transplantations

AML emerges following clonal expansion. Thus, we conducted competitive transplantation using the inducible *ERT2-Cre* model instead of the constituent hematopoietic *Vav1-Cre*, so that complete engraftment could be verified 6 weeks after transplant prior to deletion of the *Smc3* allele. In competitive transplantations, we observed a significant competitive disadvantage in the *Smc3<sup>fl/+</sup>/ERT2-Cre<sup>+/-</sup>* BM cells (Figure 5A). Endpoint analysis of BM cells also showed competitive disadvantage in the *Smc3<sup>fl/+</sup>/ERT2-Cre<sup>+/-</sup>* HSPCs and across B and T-cell lineages, implying impaired HSPC functions due to *Smc3* haploinsufficiency in the BM, and not a defect in hematopoietic peripheralization or maturation (Figure 5B–F). The competitive disadvantage was observed first in the Gr1 myeloid compartment, perhaps due to higher turn-over of these cells (Figure 5D). To verify the competitive disadvantage observed was not due to toxicity of ERT2-Cre, we repeated the competitive transplantation with the *ERT2-Cre<sup>+/-</sup>* control mice. The chimerisms of overall CD45.2+ cells and of CD45.2+ cells in all lineages were well-preserved, eliminating the possibility of ERT2-Cre toxicity (Supplemental Figure 6A–B).

The absence of pre-leukemic delayed maturation or augmented self-renewal in *Smc3* haploinsufficient mice was unexpected. Hence, we determined whether *Smc3* haploinsufficiency might increase self-renewal if it occurred in combination with specific conditions of hematopoietic stress. We again observed a competitive disadvantage in the *Smc3<sup>fl/+</sup>/ERT2-Cre<sup>+/-</sup>* BM cells following tamoxifen induction. Intriguingly, the significant myeloid competitive disadvantage was ameliorated at 18 weeks post-transplantation in the pIpC-treated group, whereas it was accelerated in the 5-fluorouracil (5-FU) treated group, although this effect was transient and by week 26 the donor cell population were equivalently reduced (Figure 5G and S5C–D).

### **Dnmt3a haploinsufficiency partially abrogated myeloid competitive disadvantage in *Smc3* haploinsufficient BM cells**

In AML patients, *DNMT3A* mutations co-occurred in approximately one-third of the cases with *SMC3* mutations that assess additional mutations.<sup>4, 5, 15, 16</sup> We therefore asked whether *Smc3* haploinsufficiency might lead to a competitive advantage if it occurred in the background of *Dnmt3a* haploinsufficiency<sup>20</sup>.

We observed that with the addition of *Dnmt3a* haploinsufficiency, the severe competitive disadvantage was partially abrogated in the *Smc3<sup>fl/+</sup>/ERT2-Cre<sup>+/-</sup>* myeloid cells, but the significant competitive disadvantage in other lineages remained intact (Figure 5A–D). The same phenotype was observed in the *Smc3<sup>fl/+</sup>/ERT2-Cre<sup>+/-</sup>/Dnmt3a<sup>+/-</sup>* BM upon endpoint analysis (Figure 5E). Accordingly, even with constitutive *Dnmt3a* haploinsufficiency, *Smc3* haploinsufficiency did not result in competitive growth advantage in hematopoietic cells.

## **Discussion**

AML is a genetically heterogeneous disease characterized by clonal expansion of immature myeloblasts, associated with recurrent mutations including the cohesin complex.<sup>25, 4, 5, 15, 16, 28</sup> Mutations in the subunits of the cohesin complex, *SMC1A*, *SMC3*, *RAD21*, and *STAG2*, have been found as early subclonal events in AML, although they are not observed in people with CHIP.<sup>5, 15, 16, 18, 19</sup> In contrast, *DNMT3A* mutations are among the most common initiating mutations in normal karyotype AML patients and the most frequently mutated genes in subjects with CHIP.<sup>25, 29</sup> Cohesin mutations are mutually exclusive of one another and fall into two general categories: mutations in *RAD21* and *STAG2* are mainly truncations and frameshifts, whereas the majority of mutations in *SMC1A* and *SMC3* are missense. In AML, cohesin mutations are not associated with genomic instability, complex karyotypes, or monosomy karyotypes, suggesting alternative pathologic mechanisms.<sup>4, 5, 15</sup>

To understand whether leukemia-associated *SMC3* missense mutations might have dominant-negative activities or phenocopy loss-of-function effects, we compared the consequences of *Smc3* deficiency and *Smc3* haploinsufficiency on murine hematopoiesis using conditionally deleted strategies. We began by validating the *Smc3* allele using whole genome sequencing, RNA-Seq, and intracellular flow cytometry, which demonstrated correct integration, splicing of approximately 50% of alleles around exon 4 leading to a frameshift mutation and an early nonsense mutation, and reduced protein levels. Our

findings suggest that leukemia-associated *SMC3* mutations are unlikely to have novel dominant negative activities because homozygous *Smc3* deletion was incompatible with embryonic (Figure 2) or adult hematopoiesis (Figure 3). In these experiments, we observed the effects first in the myeloid compartment. However, because myeloid cells have a shorter half-life than other hematopoietic cell types, the augmented temporal phenotypes observed in these cell fractions may be influenced by greater turn-over. Collectively, these studies demonstrate that *Smc3* is indispensable for embryonic and adult hematopoiesis and normal HSPC functions. Similar severe consequences for *Smc3* deficiency<sup>30</sup> and *Rad21* deficiency<sup>31</sup> have been observed, and thus cohesin genes appear to be essential in hematopoietic cells.

Leukemia-associated *SMC3* mutations are observed across all domains of the protein, and nearly one third are nonsense or splice-site variants, suggesting that many of these mutations are likely to be associated with loss of function. Therefore, we investigated the effects of *Smc3* haploinsufficiency on murine hematopoiesis. Because these mutations are associated with leukemia, we predicted that *Smc3* haploinsufficiency would augment colony forming capacity and provide hematopoietic cells a competitive advantage. However, we observed neither phenotype. Following *Smc3* haploinsufficiency induced with three different Cre models (*CMV-Cre*, *Vav1-Cre*, and *ERT2-Cre*) we observed normal CBCs, normal bone marrow hematopoietic population distributions, and normal colony forming (Figure 4A–E). We further examined expression signatures and ATAC-Seq under these steady-state conditions in *Vav1-Cre* mice where hematopoietic cells have consistently undergone heterozygous deletion and external perturbations are minimized; we observed little global dysregulation of gene expression or chromatin structure (Figure 4F–G). In both studies, internal markers (*Smc3* expression and peaks within the *Vav1* locus) served as controls and markers of the expected dynamic range.

In contrast, under conditions of chimeric competition, *Smc3* haploinsufficiency actually led to competitive disadvantage *in vivo*, with progressive population loss over time (Figure 5A–F). In these studies, *Smc3* deletion was induced using *ERT2-Cre* following a period of 6 weeks post-transplant to facilitate engraftment and stem cell homeostasis prior to deletion. Under these conditions, activation of *ERT2-Cre* alone does not lead to stem cell toxicity and competitive disadvantage (Supplemental Figure 6A–B), whereas activation of *ERT2-Cre* just prior to transplantation does.<sup>32</sup> Analysis of BM populations at the end of the study suggested reduction of populations with *Smc3* haploinsufficiency across progenitor and mature cell types, eliminating the possibility that *Smc3* haploinsufficiency led to a profound maturation block that prevented leukocyte peripheralization. The competitive disadvantage induced by somatic *Smc3* acquisition was unexpected. Therefore, we determined whether specific forms of hematopoietic stress might enable a competitive advantage that could facilitate stem cell expansion and ultimately enable leukemogenesis. We again observed a competitive disadvantage that persisted following a stem cell stressor (5-FU exposure) and an inflammatory stressor (pIpC exposure) (Figure 5G and S5C–E). Finally, because *SMC3* mutations may not be the first acquired mutation during leukemogenic chronicity, we investigated whether *Dnmt3a* haploinsufficiency might facilitate *Smc3* phenotypes. Germline *Dnmt3a* haploinsufficiency partially abrogated the myeloid competitive disadvantage of somatically acquired *Smc3* haploinsufficiency (Figure 6), suggesting that

*SMC3* mutations may require pre-existing cooperating mutations to facilitate their action. Additionally, these studies do not eliminate the possibility that the frequently observed *SMC3* missense mutations may possess novel gain-of-function activity not accessed in these *Smc3* haploinsufficient studies.

Thus, under conditions of homeostasis, where all hematopoietic cells have *Smc3* haploinsufficiency, murine *Smc3* haploinsufficiency does not appear to grossly dysregulate hematopoietic feedback mechanisms or alter normal hematopoietic maturation or self-renewal *ex vivo*. However, under conditions of competitive transplantation, we observed a disadvantage in hematopoietic cells across both myeloid and lymphoid lineages suggesting reduced cell production at a multipotent progenitor level.

These results contrast with previously published work using either knock-down strategies in CD34+ cord blood cells or using Mx1-Cre activation with pIpC. Specifically, knocking down of *Smc3* using shRNA or *RAD21* and *SMC1A* mutants have been shown to increase self-renewal in human cord blood CD34+ HSPCs *ex vivo*.<sup>33, 34</sup> *Smc3* haploinsufficiency induced by Mx1-Cre exhibited shifts in hematopoietic cell populations, colony forming, and competitive transplantation advantage when deleted using Mx1-Cre two weeks after transplantation<sup>30</sup>. These data suggest that differences in the models may interact with the biological consequences of *Smc3* reduction through yet undefined mechanisms.

In addition, It is worth noting that other MDS or AML-associated mutations such as U2AF1<sup>35, 36</sup>, SRSF2<sup>37, 38</sup>, SF3B1<sup>39, 40, 41, 42, 43</sup>, ASXL1<sup>44, 45</sup> are associated with having competitive disadvantage, which may seem counterintuitive for recurring leukemia mutations observed in patients, but appears to be recurrent biology.

The observed defects in hematopoietic cells with *Smc3* deficiency and haploinsufficiency may reflect population data from the ExAC database, where germline cohesin mutations are observed at lower than expected frequencies, suggesting a significant disadvantage in population fitness. No loss-of-function variants are detected in *SMC3*, *SMC1A*, *STAG2*, or *RAD21* (based on statistical models of case numbers and gene size, the expected numbers of loss-of-function variants were 58.5, 32, 42.7, and 21.8, respectively). Missense variants were also significantly underrepresented in *SMC3*, *SMC1A*, and *STAG2*, but not in *RAD21* ( $z = 6.25, 6.59, 5.11, \text{ and } 2.76$ ; more positive scores indicate fewer variants observed than expected). Of the published AML-associated missense mutations, only 1 is reported in ExAC (K795E occurring in 3/121,384 alleles), although synonymous changes (R155R, Q367Q, R391R), and alternative amino acid changes (N604S and I1001L) are noted.<sup>46</sup>

In recent decades, mutations in cohesin complex genes have been associated with genetic syndromes, referred to as cohesinopathies. Several important features differ between cohesinopathies and AML-associated cohesin mutations. Mutations associated with cohesinopathy tend to be in cohesin adapter proteins, such as *NILS*, *HDAC8*, and *ESCO2*, with fewer mutations observed in *SMC3*, *SMC1A*, *RAD21*, or *STAG2*.<sup>47</sup> Cohesinopathies are associated with facial dysmorphism, cognitive impairment, pre- and post-natal growth delay, and multi-organ involvement and the clinical manifestations appear milder in cases with *SMC3* and *SMC1A* mutations, compared with *NIPBL* mutations.<sup>48</sup> Hematopoietic



alterations have not been reported with cohesinopathy, nor has the development of AML. Likewise, the accumulation of aneuploidies and other chromosomal aberrations has been a recurrent feature of cohesinopathy, whereas this phenotype is largely absent in cohesin mutated AML cases, which typically present with normal karyotypes. Intriguingly, copy number gains of *STAG2* or *SMC1A* also have been associated with cohesinopathy phenotypes,<sup>49, 50, 51</sup> suggesting that there may be a critical window of adequate cohesin activity and that alterations in either direction may be detrimental. In contrast to these human data, in our mouse model, germline heterozygous *Smc3* deletion was tolerated using X-linked *CMV-Cre*, which is expressed during early embryogenesis. The heterozygous *Smc3*<sup>+/-</sup>/*CMV-Cre*<sup>+/-</sup> female progenies had no obvious developmental defects and had normal hematopoietic homeostasis in the bone marrow (Figure S3). The normal hematopoietic cell numbers and differentials in the mice reflect the maintained hematopoiesis of cohesinopathies, whereas the normal number of *Smc3* haploinsufficient pups contrasts with the near absence of cohesin mutations in the human population data. This discrepancy may be due to differences between mouse and human biology; alternatively, cohesinopathy mutations may be associated with gain of function activity not recapitulated with this allele, or activity not related directly to the SMC1A/SMC3 complex.

In summary, we did not observe evidence of impaired differentiation or augmented self-renewal *ex vivo* or *in vivo* when *Smc3* haploinsufficiency was generated using *CMV-Cre*, *ERT2-Cre*, and *Vav1-Cre*. Instead, *Smc3* haploinsufficiency was associated with competitive disadvantage, with an early bias towards phenotypes in the myeloid compartment. In AML patients, *SMC3* mutations are typically early, but not initiating, genetic events. These data also suggest that pre-existing mutations may be required to enable leukemogenic consequences of *SMC3* mutagenesis and to permit productive clonal expansion. Future studies are needed to determine the combination of cooperating mutations that predispose HSPCs to *SMC3*-induced leukemic transformation and clonal dominance.

## Methods

### Animal Studies

*Smc3*<sup>trap</sup> mice were obtained from the European Conditional Mouse Mutagenesis Program (EUCOMM) (*Smc3*<tm1a(EUCOMM)Wtsi>, MGI:4434007). To generate *Smc3*<sup>fl</sup> mice, the gene-trap was removed by crossing *Smc3*<sup>trap</sup> mice with Flp deleter mice (B6.129S4-Gt(ROSA)26Sortm2(FLP\*)Sor/J), and subsequently outbreeding the Flp allele with C57BL/6J intercrosses. We generated *Smc3* conditional deficient mice by breeding the *Smc3*<sup>fl/fl</sup> mice with *Vav1-Cre* (B6.Cg-Commd10Tg(Vav1-icre)A2Kio/J), *ERT2-Cre* (B6.Cg-Tg(cre/Esr1)5Amc/J), and *CMV-Cre* (B6.C-Tg(CMV-cre)1Cgn/J), obtained from the Jackson Laboratory. We characterized *Smc3* conditional deficient mice at 6–8 weeks old and both genders were used. Whenever possible, littermate controls were used for all experiments. CBCs were measured using Hemavet 950 (Drew Scientific Group).

All mice were on the C57BL/6 background and were cared for in the Experimental Animal Center of Washington University School of Medicine. The Washington University Animal Studies Committee approved all animal experiments.

### Intracellular Smc3 staining

Intracellular Smc3 was detected with the Pharmingen™ Transcription Factor Buffer Set (562574 BD Biosciences) according to the manufacturer's instructions. BM cells were isolated from femurs and tibias and lysed with ACK lysis buffer (150mM NH<sub>4</sub>Cl, 10mM KHCO<sub>3</sub>, 0.1mM Na<sub>2</sub>EDTA [Na<sub>2</sub>ethylenediaminetetraacetic acid], PH7.2–7.4). Cells were stained with cell-surface markers to identify cell type by flow cytometry and then fixed for 40 minutes at 4°C. Cells were washed with perm wash buffer and incubated with primary antibody against Smc3 (1:100 dilution, ab9263, Abcam) for 30 minutes at 4°C. Cells were washed in perm wash buffer and incubated in secondary antibody (1:500 dilution, chicken anti-rabbit Alexa Fluor 647, Molecular Probes) for 30 minutes at 4°C. Cells were rinsed in perm wash buffer and analyzed by flow cytometry. The mean fluorescence intensity was calculated for the AF647 signal.

### Flow cytometry

After lysis of red blood cells by ACK lysis buffer, peripheral blood, BM, spleen cells, or thymocytes were treated with anti-mouse CD16/32 (eBioscience; clone 93) and stained with the indicated combinations of the following antibodies (all antibodies are from eBioscience unless noted otherwise): CD34 FITC (clone RAM34), CD11b PE (clone M1/70), c-Kit PECy7 (clone 2B8) or BV421 (BioLegend, clone 2B8), Sca1 PE-Dazzle™ 594 (BioLegend, clone D7) or APC (clone D7), Gr-1 FITC, PECy7, APC (clone RB6–8C5), or BV421 (BioLegend, clone RB6–8C5), B220 PE, PECy7, APC (clone RA3–6B2), or APC-Cy7 (BioLegend, clone RA3–6B2), CD3 PECy7 (clone 145–2C11), CD71 PE(clone R17217), Ter-119 PECy7 or APC (clone TER-119), CD16/32 BV510 (clone 93), CD150 PE (BioLegend 115903, clone TC15–12F12.2), CD48 APC-Cy7 (BioLegend, clone HM48–1), Ly5.1 APC (clone A20) or AF700 (BioLegend, clone A20), Ly 5.2 PE or e450 (clone 104). The following flow phenotypes were used for stem and progenitor cell flow: Lin- (lineage negative): B220-, CD3e-, Gr-1-, Ter-119-, CD4-, CD8-, CD19-, CD127-; KL: Lin-, cKit+, Sca1-; KLS: Lin-, cKit+, Sca-1+; KLS-SLAM: Lin-, cKit+, Sca-1+, CD150+, CD48-; GMP: Lin-, cKit+, Sca-1-, CD34+, CD16/32+; CMP: Lin-, cKit+, Sca-1-, CD34+, CD16/32-; and MEP: Lin-, cKit+, Sca-1-, CD34-, CD16/32-.

Analysis was performed using a FACScan (Beckman Coulter) or Gallios flow cytometer (Beckman Coulter). Cell sorting was performed using I-Cyt Synergy II sorter (I-Cyt Technologies). Flow cytometry data were analyzed with FlowJo Software Version 10 (TreeStar), Excel (Microsoft), and Prism 7.02 (GraphPad Software).

### Competitive transplantation

Competitive transplantation was performed using  $0.5 \times 10^6$  whole BM cells from indicated donor mice (CD45.2) mixed with  $0.5 \times 10^6$  competitor whole BM cells wild-type CD45.1 (Ly5.1)  $\times$  CD45.2 mice. Mixture cells were injected intravenously into 6–8 weeks old CD45.1 recipient mice that received 1,100 cGy total body irradiation (Mark 1 Cesium irradiator, J.L. Shepard) 24 hours prior to transplantation. For *Smc3<sup>fl/fl</sup>/ERT2-Cre<sup>+/-</sup>* or *Smc3<sup>fl/+</sup>/ERT2-Cre<sup>+/-</sup>* transplantation, recipient mice were treated with tamoxifen (dissolved in sterile corn oil, Sigma-Aldrich) 6 weeks post-transplant via oral gavage for 9 doses (3 mg/day/mouse, 3 days/week). Peripheral blood was examined for donor cell chimerism at

indicated time points after transplantation. Recipient mice BM were analyzed at the end of experiment.

### Colony replating assay

BM cells were harvested and plated in duplicate (10,000 BM cells/plate) in complete mouse methylcellulose medium with stem cell factor, IL-3, IL-6, and Epo (R&D Systems). Colonies were counted on day 7, and cells were collected from methylcellulose in warm Dulbecco modified Eagle medium containing 2% fetal bovine serum, washed, and replated as before. An aliquot of cells was taken for analysis of myeloid (Gr1, CD11b) and mast cell markers (cKit, FcER1) by flow cytometry. This process was repeated for 4 weeks or until colony formation failed.

### RNA sequencing of multipotent progenitors and analysis

Multipotent progenitors (KLS; Lin<sup>-</sup>, cKit<sup>+</sup>, Sca1<sup>-</sup>) were sorted from three wild-type or *Smc3<sup>fl/+</sup>/Vav1-Cre<sup>+/-</sup>* mice into DMEM media. Flow cytometry of samples after sorting validated >93% sort accuracy. RNA was extracted from cell pellets using a miRNeasy kit (QIAGEN) and genomic DNA was removed by RNase-Free DNase Set (QIAGEN). RNA was analyzed for degradation using the RNA Nano Chip (Agilent #5067–1521). An input of 300ng was taken forward for each sample using the TruSeq Stranded Total RNA with Ribo-Zero Globin Kit (Illumina #20020612). Final Libraries were analyzed using the High Sensitivity DNA Chip (Agilent# 5067–4626). All Libraries were pooled and run across 3 lanes of HiSeq4000. RNAseq data were aligned to the human reference with Tophat v2.0.8 (denovo mode, params: --library-type frfirststrand --bowtie-version=2.1.0). Expression levels were calculated with Cufflinks v2.1.1 (params: --max-bundle-length 10000000 --max-bundle-frags 10000000).<sup>52</sup>

### ATAC-Sequencing of multipotent progenitor and analysis

Chromatin accessibility assays using the bacterial Tn5 transposase were performed using multipotent progenitors (KLS; Lin<sup>-</sup>, cKit<sup>+</sup>, Sca1<sup>-</sup>) sorted from *Smc3<sup>fl/+</sup>* or *Smc3<sup>fl/+</sup>/Vav1-Cre<sup>+/-</sup>* mice in triplicate. DNA was prepared from 75,000 sorted cells and >93% sorting accuracy verified with post-sort analysis. ATAC libraries were generated exactly as described<sup>53</sup> and pooled and sequenced on a HiSeqX instrument (Illumina) to obtain between 133 and 152 million 2×150 bp paired-end reads. Raw sequencing reads were adapter trimmed with trim galore using cutadapt version 1.8.1 (Martin EMBnet 2011) and then aligned to the mouse reference genome (mm10) using bwa mem (Li H. arXiv:1303.3997v1 (2013)). Peaks in each sample were identified with macs2<sup>54</sup> using the -f BAMPE parameter and then filtered to retain peaks with a q-value <0.01. Peak summits from all samples were merged together with BEDtools merge<sup>55</sup> using parameters to combine summits within 50 bp of each other. Read counts at the merged peak summits were obtained for all samples using the deepTools multiBamSummary command<sup>56</sup> with the minimum mapping quality set to 1, and then processed using DESeq2<sup>57</sup> with default parameters to obtain normalized counts for each peak summit and to perform differential analysis across all peaks between wild-type and mutant mice.

## Statistics

Statistical analysis was performed using Prism 7.02 (GraphPad Software) and Excel (Microsoft). Unpaired two-tailed *t*-test, one-way, and two-way ANOVA with Turkey's multiple comparisons tests were performed, as appropriate. *P* values < 0.05 were considered statistically significant. Error bars represent standard deviation. Data points without error bars have standard deviation below Prism 7.02's limit to display.

## Supplementary Material

Refer to Web version on PubMed Central for supplementary material.

## Acknowledgments

This work was supported by a V Foundation Scholar award (JSW) and NCI AML-SPORE (P50 CA171963). We thank Deborah Laflamme and Conner York for excellent animal husbandry support. We thank Nicole Helton for technical assistance with library construction and Dr. David Spencer for providing assistance with ATAC-Seq analysis. We thank Dr. Timothy J. Ley and Dr. Grant A. Challen for critically reading the manuscript.

## References

1. Saultz JN, Garzon R. Acute Myeloid Leukemia: A Concise Review. *J Clin Med*. 2016;5(3). doi: 10.3390/jcm5030033
2. Lagunas-Rangel FA, Chávez-Valencia V, Gómez-Guijosa MÁ, Cortes-Penagos C. Acute Myeloid Leukemia—Genetic Alterations and Their Clinical Prognosis. *Int J Hematol-Oncol Stem Cell Res*. 2017;11(4):328–339. [PubMed: 29340131]
3. Cancer Genome Atlas Research Network, Ley TJ, Miller C, et al. Genomic and epigenomic landscapes of adult de novo acute myeloid leukemia. *N Engl J Med*. 2013;368(22):2059–2074. doi: 10.1056/NEJMoa1301689 [PubMed: 23634996]
4. Kon A, Shih L-Y, Minamino M, et al. Recurrent mutations in multiple components of the cohesin complex in myeloid neoplasms. *Nat Genet*. 2013;45(10):1232–1237. doi:10.1038/ng.2731 [PubMed: 23955599]
5. Thota S, Viny AD, Makishima H, et al. Genetic alterations of the cohesin complex genes in myeloid malignancies. *Blood*. 2014;124(11):1790–1798. doi:10.1182/blood-2014-04-567057 [PubMed: 25006131]
6. Yoshida K, Toki T, Okuno Y, et al. The landscape of somatic mutations in Down syndrome–related myeloid disorders. *Nat Genet*. 2013;45(11):1293–1299. doi:10.1038/ng.2759 [PubMed: 24056718]
7. Barber TD, McManus K, Yuen KWY, et al. Chromatid cohesion defects may underlie chromosome instability in human colorectal cancers. *Proc Natl Acad Sci*. 2008;105(9):3443–3448. doi:10.1073/pnas.0712384105 [PubMed: 18299561]
8. Goringe KL, Ramakrishna M, Williams LH, et al. Are there any more ovarian tumor suppressor genes? A new perspective using ultra high-resolution copy number and loss of heterozygosity analysis. *Genes Chromosomes Cancer*. 2009;48(10):931–942. doi:10.1002/gcc.20694 [PubMed: 19603523]
9. Bailey ML, O'Neil NJ, Pel DM van, Solomon DA, Waldman T, Hieter P. Glioblastoma Cells Containing Mutations in the Cohesin Component STAG2 Are Sensitive to PARP Inhibition. *Mol Cancer Ther*. 2014;13(3):724–732. doi:10.1158/1535-7163.MCT-13-0749 [PubMed: 24356817]
10. Solomon DA, Kim J-S, Bondaruk J, et al. Frequent truncating mutations of *STAG2* in bladder cancer. *Nat Genet*. 2013;45(12):1428–1430. doi:10.1038/ng.2800 [PubMed: 24121789]
11. Balbás-Martínez C, Sagrera A, Carrillo-de-Santa-Pau E, et al. Recurrent inactivation of *STAG2* in bladder cancer is not associated with aneuploidy. *Nat Genet*. 2013;45(12):1464–1469. doi: 10.1038/ng.2799 [PubMed: 24121791]

12. Solomon DA, Kim T, Diaz-Martinez LA, et al. Mutational Inactivation of STAG2 Causes Aneuploidy in Human Cancer. *Science*. 2011;333(6045):1039–1043. doi:10.1126/science.1203619 [PubMed: 21852505]
13. Remeseiro S, Cuadrado A, Gómez-López G, Pisano DG, Losada A. A unique role of cohesin-SA1 in gene regulation and development. *EMBO J*. 2012;31(9):2090–2102. doi:10.1038/emboj.2012.60 [PubMed: 22415368]
14. Mannini L, Cucco F, Quarantotti V, Krantz ID, Musio A. Mutation spectrum and genotype-phenotype correlation in Cornelia de Lange syndrome. *Hum Mutat*. 2013;34(12):1589–1596. doi:10.1002/humu.22430 [PubMed: 24038889]
15. Welch JS, Ley TJ, Link DC, et al. The Origin and Evolution of Mutations in Acute Myeloid Leukemia. *Cell*. 2012;150(2):264–278. doi:10.1016/j.cell.2012.06.023 [PubMed: 22817890]
16. Thol F, Bollin R, Gehlhaar M, et al. Mutations in the cohesin complex in acute myeloid leukemia: clinical and prognostic implications. *Blood*. 2014;123(6):914–920. doi:10.1182/blood-2013-07-518746 [PubMed: 24335498]
17. Conese M, Liso A. Cohesin complex is a major player on the stage of leukemogenesis. *Stem Cell Investig*. 2016;3:18. doi:10.21037/sci.2016.05.04
18. Xie M, Lu C, Wang J, et al. Age-related mutations associated with clonal hematopoietic expansion and malignancies. *Nat Med*. 2014;20(12):1472–1478. doi:10.1038/nm.3733 [PubMed: 25326804]
19. Jaiswal S, Natarajan P, Silver AJ, et al. Clonal Hematopoiesis and Risk of Atherosclerotic Cardiovascular Disease. *N Engl J Med*. 2017;377(2):111–121. doi:10.1056/NEJMoa1701719 [PubMed: 28636844]
20. Cole CB, Russler-Germain DA, Ketkar S, et al. Haploinsufficiency for DNA methyltransferase 3A predisposes hematopoietic cells to myeloid malignancies. *J Clin Invest*. 2017;127(10):3657–3674. doi:10.1172/JCI93041 [PubMed: 28872462]
21. Ball AR, Chen Y-Y, Yokomori K. Mechanisms of cohesin-mediated gene regulation and lessons learned from cohesinopathies. *Biochim Biophys Acta BBA - Gene Regul Mech*. 2014;1839(3):191–202. doi:10.1016/j.bbarm.2013.11.002
22. Wendt KS, Yoshida K, Itoh T, et al. Cohesin mediates transcriptional insulation by CCCTC-binding factor. *Nature*. 2008;451(7180):796–801. doi:10.1038/nature06634 [PubMed: 18235444]
23. Merkenschlager M, Odom DT. CTCF and cohesin: linking gene regulatory elements with their targets. *Cell*. 2013;152(6):1285–1297. doi:10.1016/j.cell.2013.02.029 [PubMed: 23498937]
24. Schmidt D, Schwalie PC, Ross-Innes CS, et al. A CTCF-independent role for cohesin in tissue-specific transcription. *Genome Res*. 2010;20(5):578–588. doi:10.1101/gr.100479.109 [PubMed: 20219941]
25. Genomic and Epigenomic Landscapes of Adult De Novo Acute Myeloid Leukemia. *N Engl J Med*. 2013;368(22):2059–2074. doi:10.1056/NEJMoa1301689 [PubMed: 23634996]
26. Tusher VG, Tibshirani R, Chu G. Significance analysis of microarrays applied to the ionizing radiation response. *Proc Natl Acad Sci U S A*. 2001;98(9):5116–5121. doi:10.1073/pnas.091062498 [PubMed: 11309499]
27. Kanehisa M, Sato Y, Kawashima M, Furumichi M, Tanabe M. KEGG as a reference resource for gene and protein annotation. *Nucleic Acids Res*. 2016;44(D1):D457–D462. doi:10.1093/nar/gkv1070 [PubMed: 26476454]
28. Walter MJ, Shen D, Ding L, et al. Clonal Architecture of Secondary Acute Myeloid Leukemia. *N Engl J Med*. 2012;366(12):1090–1098. doi:10.1056/NEJMoa1106968 [PubMed: 22417201]
29. Genovese G, Kähler AK, Handsaker RE, et al. Clonal Hematopoiesis and Blood-Cancer Risk Inferred from Blood DNA Sequence. *N Engl J Med*. 2014;371(26):2477–2487. doi:10.1056/NEJMoa1409405 [PubMed: 25426838]
30. Viny AD, Ott CJ, Spitzer B, et al. Dose-dependent role of the cohesin complex in normal and malignant hematopoiesis. *J Exp Med*. 2015;212(11):1819–1832. doi:10.1084/jem.20151317 [PubMed: 26438361]
31. Xu H, Balakrishnan K, Malaterre J, et al. Rad21-cohesin haploinsufficiency impedes DNA repair and enhances gastrointestinal radiosensitivity in mice. *PloS One*. 2010;5(8):e12112. doi:10.1371/journal.pone.0012112 [PubMed: 20711430]

32. Welch JS, Yuan W, Ley TJ. PML-RARA can increase hematopoietic self-renewal without causing a myeloproliferative disease in mice. *J Clin Invest*. 2011;121(4):1636–1645. doi:10.1172/JCI42953 [PubMed: 21364283]
33. Mullenders J, Aranda-Orgilles B, Lhoumaud P, et al. Cohesin loss alters adult hematopoietic stem cell homeostasis, leading to myeloproliferative neoplasms. *J Exp Med*. 2015;212(11):1833–1850. doi:10.1084/jem.20151323 [PubMed: 26438359]
34. Mazumdar C, Shen Y, Xavy S, et al. Leukemia-Associated Cohesin Mutants Dominantly Enforce Stem Cell Programs and Impair Human Hematopoietic Progenitor Differentiation. *Cell Stem Cell*. 2015;17(6):675–688. doi:10.1016/j.stem.2015.09.017 [PubMed: 26607380]
35. Shirai CL, Ley JN, White BS, et al. Mutant U2AF1 Expression Alters Hematopoiesis and Pre-mRNA Splicing In Vivo. *Cancer Cell*. 2015;27(5):631–643. doi:10.1016/j.ccell.2015.04.008 [PubMed: 25965570]
36. Fei DL, Zhen T, Durham B, et al. Impaired hematopoiesis and leukemia development in mice with a conditional knock-in allele of a mutant splicing factor gene U2af1. *Proc Natl Acad Sci U S A*. 2018;115(44):E10437–E10446. doi:10.1073/pnas.1812669115 [PubMed: 30322915]
37. Kim E, Ilagan JO, Liang Y, et al. SRSF2 Mutations Contribute to Myelodysplasia by Mutant-Specific Effects on Exon Recognition. *Cancer Cell*. 2015;27(5):617–630. doi:10.1016/j.ccell.2015.04.006 [PubMed: 25965569]
38. Komeno Y, Huang Y-J, Qiu J, et al. SRSF2 Is Essential for Hematopoiesis, and Its Myelodysplastic Syndrome-Related Mutations Dysregulate Alternative Pre-mRNA Splicing. *Mol Cell Biol*. 2015;35(17):3071–3082. doi:10.1128/MCB.00202-15 [PubMed: 26124281]
39. Wang C, Sashida G, Saraya A, et al. Depletion of Sf3b1 impairs proliferative capacity of hematopoietic stem cells but is not sufficient to induce myelodysplasia. *Blood*. 2014;123(21):3336–3343. doi:10.1182/blood-2013-12-544544 [PubMed: 24735968]
40. Matsunawa M, Yamamoto R, Sanada M, et al. Haploinsufficiency of Sf3b1 leads to compromised stem cell function but not to myelodysplasia. *Leukemia*. 2014;28(9):1844–1850. doi:10.1038/leu.2014.73 [PubMed: 24535406]
41. Visconte V, Tabarrok A, Zhang L, et al. Splicing factor 3b subunit 1 (Sf3b1) haploinsufficient mice display features of low risk Myelodysplastic syndromes with ring sideroblasts. *J Hematol Oncol J Hematol Oncol*. 2014;7:89. doi:10.1186/s13045-014-0089-x [PubMed: 25481243]
42. Obeng EA, Chappell RJ, Seiler M, et al. Physiologic Expression of Sf3b1(K700E) Causes Impaired Erythropoiesis, Aberrant Splicing, and Sensitivity to Therapeutic Spliceosome Modulation. *Cancer Cell*. 2016;30(3):404–417. doi:10.1016/j.ccell.2016.08.006 [PubMed: 27622333]
43. Mupo A, Seiler M, Sathiaseelan V, et al. Hemopoietic-specific Sf3b1-K700E knock-in mice display the splicing defect seen in human MDS but develop anemia without ring sideroblasts. *Leukemia*. 2017;31(3):720–727. doi:10.1038/leu.2016.251 [PubMed: 27604819]
44. Abdel-Wahab O, Gao J, Adli M, et al. Deletion of Asx11 results in myelodysplasia and severe developmental defects in vivo. *J Exp Med*. 2013;210(12):2641–2659. doi:10.1084/jem.20131141 [PubMed: 24218140]
45. Nagase R, Inoue D, Pastore A, et al. Expression of mutant Asx11 perturbs hematopoiesis and promotes susceptibility to leukemic transformation. *J Exp Med*. 2018;215(6):1729–1747. doi:10.1084/jem.20171151 [PubMed: 29643185]
46. ExAC Browser. <http://exac.broadinstitute.org/gene/ENSG00000108055>. Accessed May 18, 2018.
47. Cucco F, Musio A. Genome stability: What we have learned from cohesinopathies. *Am J Med Genet C Semin Med Genet*. 2016;172(2):171–178. doi:10.1002/ajmg.c.31492 [PubMed: 27091086]
48. Ramos FJ, Puisac B, Baquero-Montoya C, et al. Clinical utility gene card for: Cornelia de Lange syndrome. *Eur J Hum Genet*. 2015;23(10):1431. doi:10.1038/ejhg.2014.270
49. Kumar R, Corbett MA, Van Bon BWM, et al. Increased STAG2 dosage defines a novel cohesinopathy with intellectual disability and behavioral problems. *Hum Mol Genet*. 2015;24(25):7171–7181. doi:10.1093/hmg/ddv414 [PubMed: 26443594]

50. Leroy C, Jacquemont M-L, Doray B, et al. Xq25 duplication: the crucial role of the STAG2 gene in this novel human cohesinopathy. *Clin Genet.* 2016;89(1):68–73. doi:10.1111/cge.12567 [PubMed: 25677961]
51. Baquero-Montoya C, Gil-Rodríguez MC, Teresa-Rodrigo ME, et al. Could a patient with SMC1A duplication be classified as a human cohesinopathy? *Clin Genet.* 2014;85(5):446–451. doi:10.1111/cge.12194 [PubMed: 23683030]
52. Trapnell C, Roberts A, Goff L, et al. Differential gene and transcript expression analysis of RNA-seq experiments with TopHat and Cufflinks. *Nat Protoc.* 2012;7(3):562–578. doi:10.1038/nprot.2012.016 [PubMed: 22383036]
53. Buenrostro JD, Giresi PG, Zaba LC, Chang HY, Greenleaf WJ. Transposition of native chromatin for fast and sensitive epigenomic profiling of open chromatin, DNA-binding proteins and nucleosome position. *Nat Methods.* 2013;10(12):1213–1218. doi:10.1038/nmeth.2688 [PubMed: 24097267]
54. Zhang Y, Liu T, Meyer CA, et al. Model-based analysis of ChIP-Seq (MACS). *Genome Biol.* 2008;9(9):R137. doi:10.1186/gb-2008-9-9-r137 [PubMed: 18798982]
55. Quinlan AR, Hall IM. BEDTools: a flexible suite of utilities for comparing genomic features. *Bioinforma Oxf Engl.* 2010;26(6):841–842. doi:10.1093/bioinformatics/btq033
56. Ramírez F, Dündar F, Diehl S, Grüning BA, Manke T. deepTools: a flexible platform for exploring deep-sequencing data. *Nucleic Acids Res.* 2014;42(Web Server issue):W187–191. doi:10.1093/nar/gku365 [PubMed: 24799436]
57. Love MI, Huber W, Anders S. Moderated estimation of fold change and dispersion for RNA-seq data with DESeq2. *Genome Biol.* 2014;15(12):550. doi:10.1186/s13059-014-0550-8 [PubMed: 25516281]

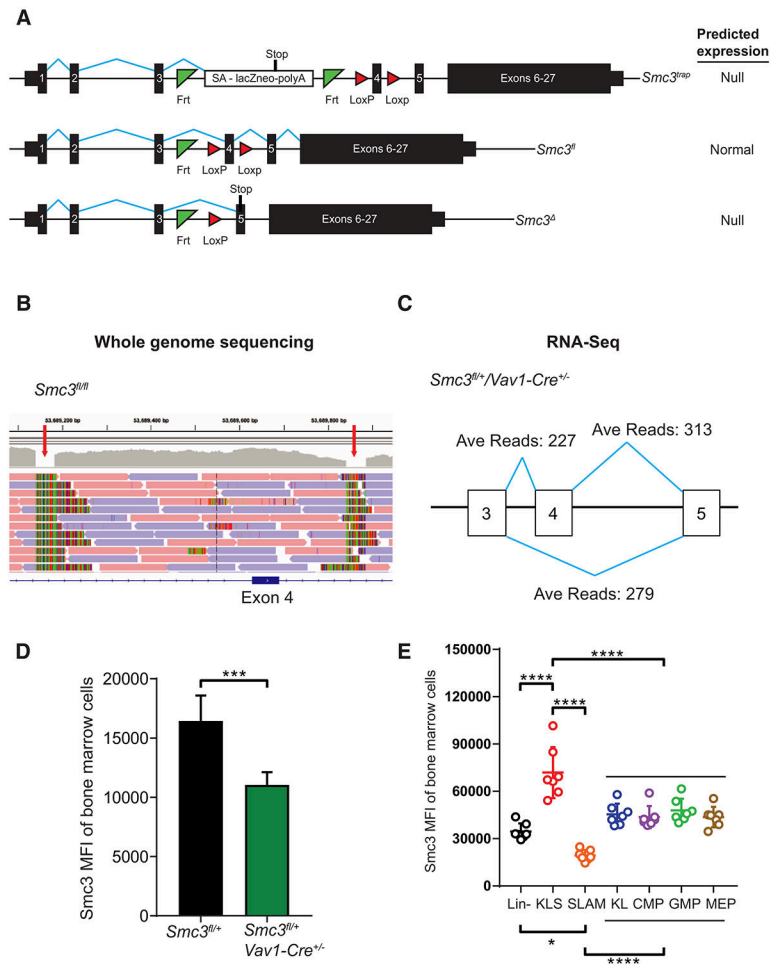


**Figure 1. Generation of *Smc3* conditional deficient mice and allele validation.**

(A) *Smc3* haploinsufficient mouse model (*Smc3<sup>trap/+</sup>*) was obtained from the European Mouse Mutagenesis Program (EUCOMM). *Smc3* conditionally deficient mice were generated by removing the gene-trap cassette, which retains the loxP sites flanking exon 4 (*Smc3<sup>fl/+</sup>*) and crossing these mice with either *Vav1-Cre<sup>+/-</sup>* or *ERT2-Cre<sup>+/-</sup>* to delete the allele (*Smc3<sup>-/-</sup>*). All mice are on the C57BL/6J background. (B) Whole genome sequencing validation of *Smc3<sup>fl</sup>* integration sites. (C) RNA-Seq data of the *Smc3<sup>fl/+</sup>/Vav1-Cre<sup>+/-</sup>* mice showed 227 transcripts spliced from exon 3 to 4 and then 313 transcripts from exon 4 to 5 while 279 transcripts from the other allele spliced from exon 3 to 5 (average data from 3 mice). (D) *Smc3* haploinsufficiency was confirmed by reduced *Smc3* level in the bone marrow (BM) cells of the *Smc3<sup>fl/+</sup>/Vav1-Cre<sup>+/-</sup>* mice measured using intracellular flow cytometry (n=5). \*Denotes statistical significance by t-test. \*\*\* $p < 0.001$ . (E) *Smc3* level is significantly higher in KLS (Lin-cKit+Sca1+) cells and progenitor populations than Lin- and SLAM (Lin-cKit+Sca1+CD48-CD150+). \*Denotes statistical significance by one-way ANOVA with Turkey's multiple comparisons test. \*\*\* $p < 0.0001$ .



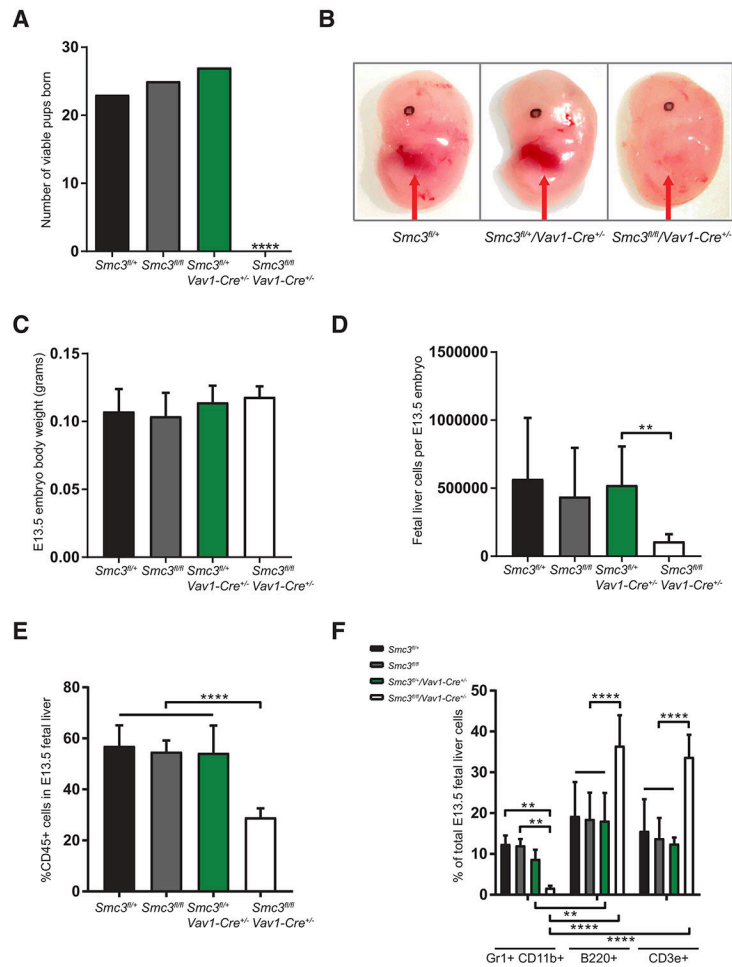


### Figure 2. Embryonic hematopoietic *Smc3* deletion.

(A) No *Smc3<sup>fl/fl</sup>/Vav1-Cre<sup>+/-</sup>* pups were observed following *Smc3<sup>fl/fl</sup>* and *Smc3<sup>fl/fl</sup>/Vav1-Cre<sup>+/-</sup>* intercrosses (n=11 litters). \*Denotes statistical significance by Chi-square test. \*\*\*\* $p < 0.0001$ . The E13.5 *Smc3<sup>fl/fl</sup>/Vav1-Cre<sup>+/-</sup>* embryos (B) lacked gross fetal livers but retain (C) normal body weight compared with littermates. (D) The E13.5 *Smc3<sup>fl/fl</sup>/Vav1-Cre<sup>+/-</sup>* embryos had decreased total fetal liver cells and (E) fetal liver hematopoietic cells (CD45.2+). (F) Myeloid (Gr1+CD11b+) cells were reduced and increased proportions of B220+ and CD3e+ lymphocytes were observed in E13.5 *Smc3<sup>fl/fl</sup>/Vav1-Cre<sup>+/-</sup>* fetal livers compared to littermate controls. (C-F) n=7 embryos per group, \*Denotes statistical significance by one-way (D-E) and two-way (F) ANOVA with Turkey's multiple comparisons test. \*\* $p < 0.01$ , \*\*\*\* $p < 0.0001$ .

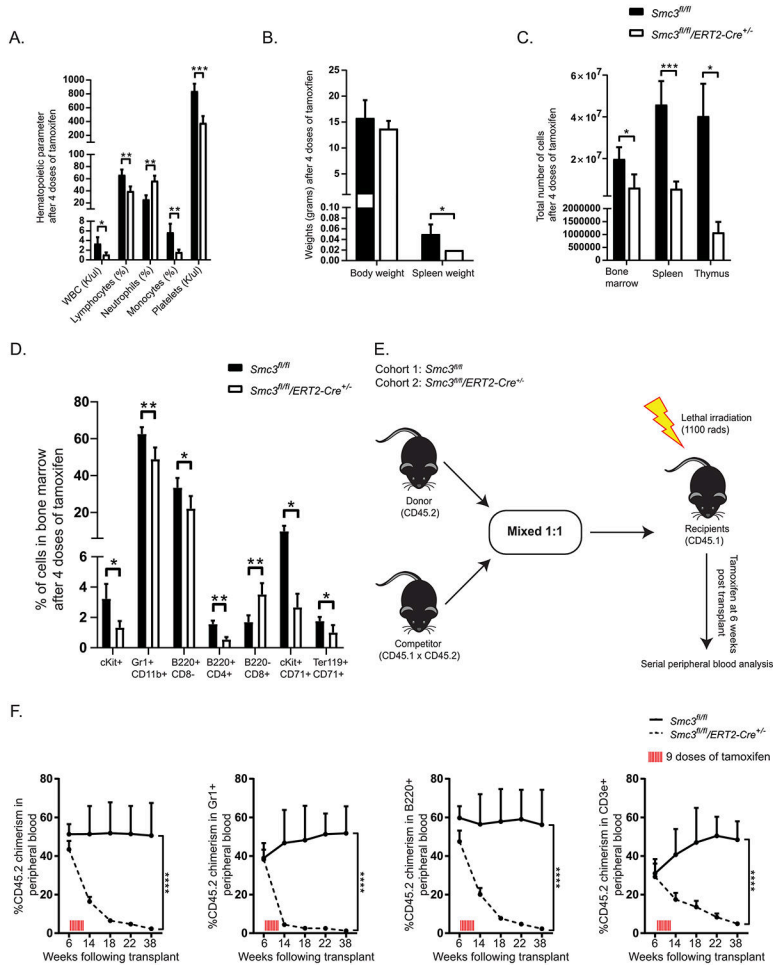


**Figure 3. Homozygous somatic *Smc3* deletion.**

(A)  $Smc3^{fl/fl}/ERT2-Cre^{+/-}$  and  $Smc3^{fl/fl}$  littermate control mice were treated with 4 doses of tamoxifen (3 mg orally on days 1<sup>st</sup>, 3<sup>rd</sup>, 5<sup>th</sup>, 8<sup>th</sup> and analyzed on day 8, n = 4 mice in each group) (A) Peripheral blood analysis. (B) Body weight and spleen weight. (C) Total number of cells in the bone marrow, spleen, and thymus. (D) Analysis of lineage percentages within total bone marrow cells. (A-D) n=4 mice per group, \*Denotes statistical significance by t-test. \* $p < 0.05$ , \*\* $p < 0.01$ , \*\*\* $p < 0.001$ . (E) Experimental schema of the  $Smc3^{fl/fl}/ERT2-Cre^{+/-}$  competitive transplantation. (F) Recipient mice were treated with tamoxifen after 6-week engraftment. After tamoxifen-mediated deletion, *Smc3* deficient cells were rapidly outcompeted, with earliest cell loss in the Gr1+ myeloid compartment, showing as complete competitive disadvantage. \*Denotes statistical significance by 2-way ANOVA with Turkey’s multiple comparisons test. \*\*\* $p < 0.0001$ . (E-F) n=10 mice per group.

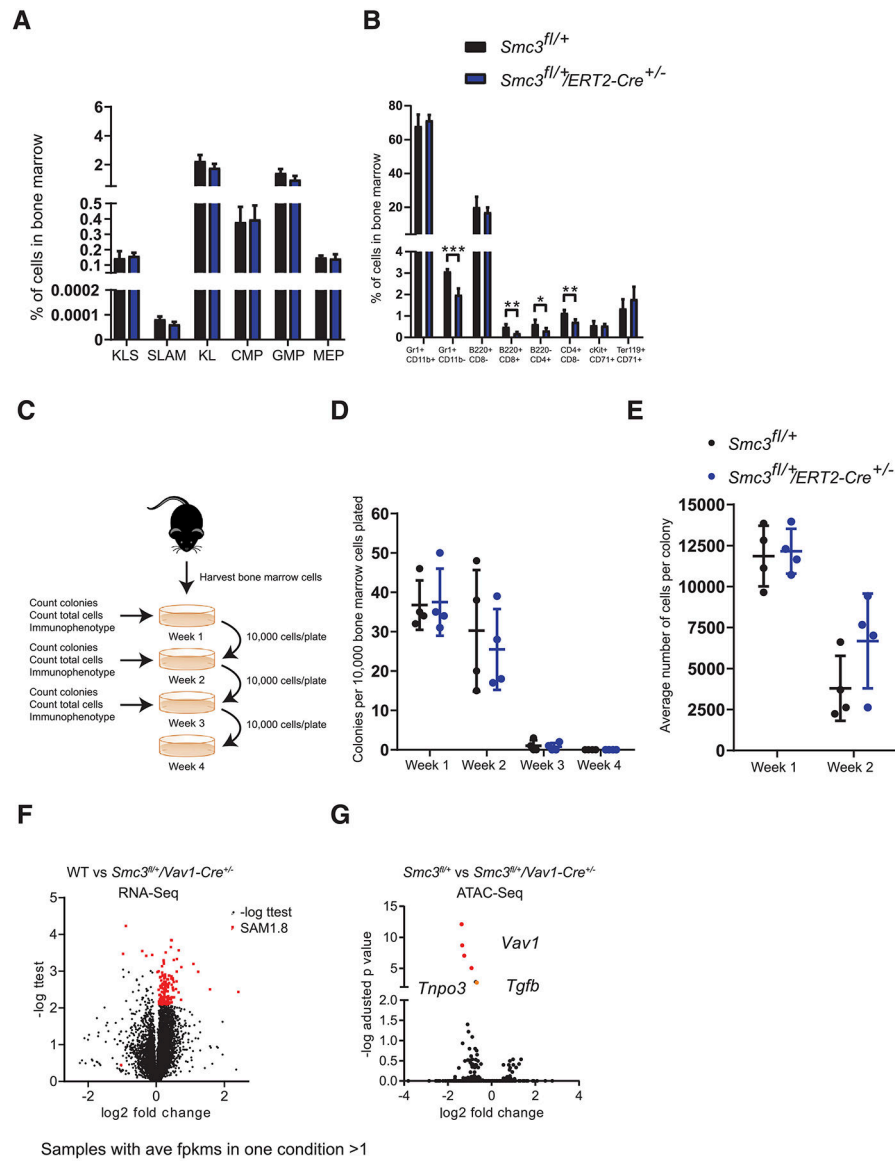


#### Figure 4. Hematopoietic *Smc3* haploinsufficiency.

(A and B) Distribution of bone marrow stem, progenitor, and lineage populations in *Smc3<sup>fl/+</sup>/ERT2-Cre<sup>+/-</sup>* and littermate *Smc3<sup>fl/+</sup>* mice following 9 doses of tamoxifen (n=6 mice per group). (C) Experimental schema of serial replating assay. (D-E) Colony numbers and average cells per colony on indicated week of plating in methylcellulose (n=4 mice per group). \*Denotes statistical significance by t-test. \* $p < 0.05$ , \*\* $p < 0.01$ . (F) Expression analysis by RNA-Seq data of KL (Lin-cKit+Sca1-) bone marrow cells from *Smc3<sup>fl/+</sup>/Vav1-Cre<sup>+/-</sup>* compared to wild-type cells (n=3 mice per group). (G) Comparison of relative peak intensity identified by ATAC-Seq of KL bone marrow cells from relative peak *Smc3<sup>fl/+</sup>/Vav1-Cre<sup>+/-</sup>* compared to wild-type cells (n=3 mice per group)

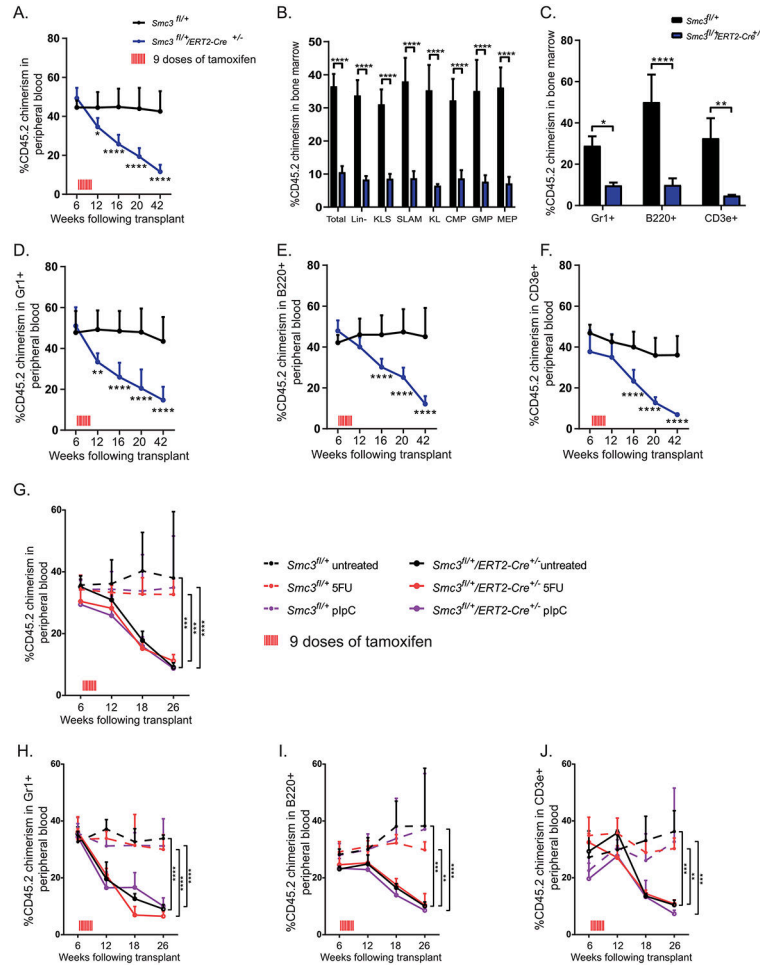


**Figure 5. Competitive transplantation of *Smc3* haploinsufficient bone marrow cells.** (A-F) Competitive repopulation assay using *Smc3*<sup>fl/+</sup>/*ERT2-Cre*<sup>+/-</sup> BM cells and littermate *Smc3*<sup>fl/+</sup> BM cells with competitor CD45.1 × CD45.2 bone marrow cells (3 donor mice per group and 10 recipient mice per group). Following 6 weeks of engraftment, equal peripheral chimerism was validated and recipient mice were treated with 9 doses of tamoxifen. (B - C) Following 42 weeks, bone marrow chimerism was analyzed (n=3 mice per group). \*Denotes statistical significance by t-test, \**p*<0.05, \*\**p*<0.01, \*\*\*\**p*<0.0001. (D-F) At interval time-points during follow-up peripheral blood chimerism was evaluated within the Gr1, B220, and CD3e compartments. \*Denotes statistical significance by 2-way ANOVA with Turkey’s multiple comparisons test, \**p*<0.05, \*\**p*<0.01, \*\*\*\**p*<0.0001. (G-J) Competitive repopulation assay of *Smc3*<sup>fl/+</sup>/*ERT2-Cre*<sup>+/-</sup> BM cells under hematopoietic stresses (n=10). As before, recipient mice were treated with 9 doses of tamoxifen after 6-week engraftment. PIpC and 5-FU were given 16 weeks post-transplant, respectively. \*Denotes statistical significance by 2-way ANOVA with Turkey’s multiple comparisons test, \*\**p*<0.01, \*\*\**p*<0.001, \*\*\*\**p*<0.0001.

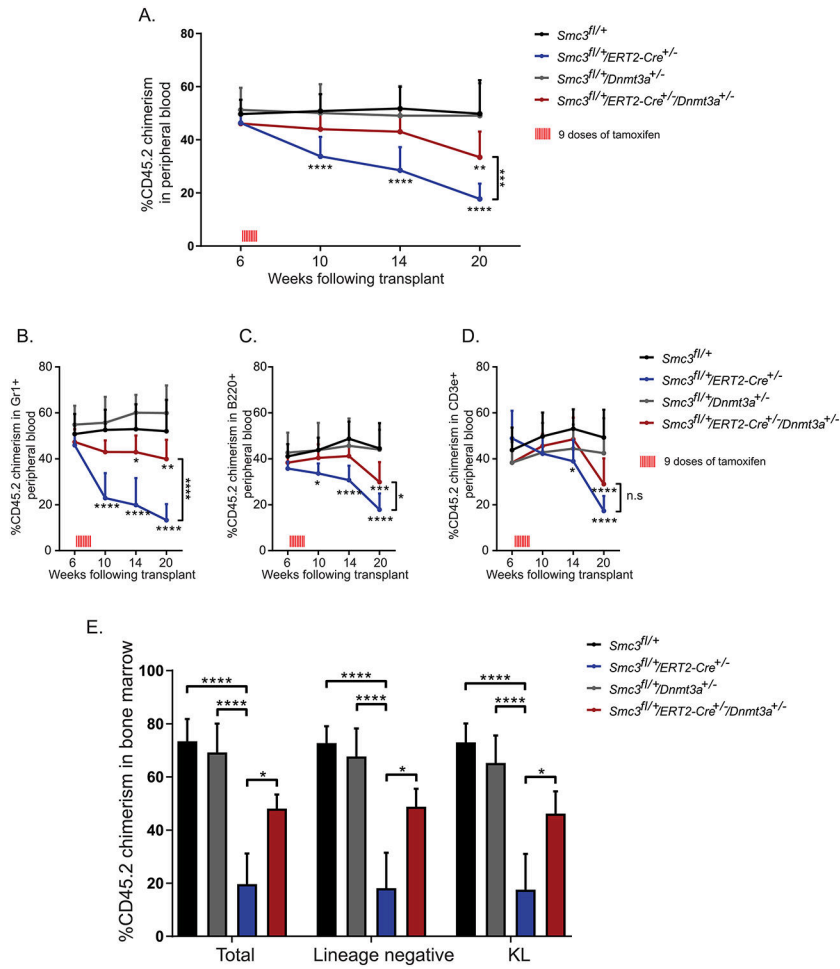


**Figure 6. Effect of *Dnmt3a* haploinsufficiency on competitive disadvantage in *Smc3* haploinsufficient BM cells.**

(A-D) Competitive repopulation assay of *Smc3<sup>fl/+</sup>/ERT2-Cre<sup>+/-</sup>/Dnmt3a<sup>+/-</sup>* BM cells and indicated littermate controls (n=10 mice per group). As in Figure 5, total bone marrow cells were allowed to engraft for 6 weeks and equivalent chimerism was validated before treatment of all cohorts with 9 doses of tamoxifen (3 mg/day). Peripheral blood chimerism was evaluated by flow cytometry at indicated time points. (E) Bone marrow chimerism assessed by flow cytometry 26 weeks after engraftment. KL: Lin-cKit+Sca1-. (n=4 mice in each group). \*Denotes statistical significance by 2-way ANOVA with Turkey’s multiple comparisons test. \**p*<0.05, \*\**p*<0.01, \*\*\**p*<0.001, \*\*\*\**p*<0.0001.